

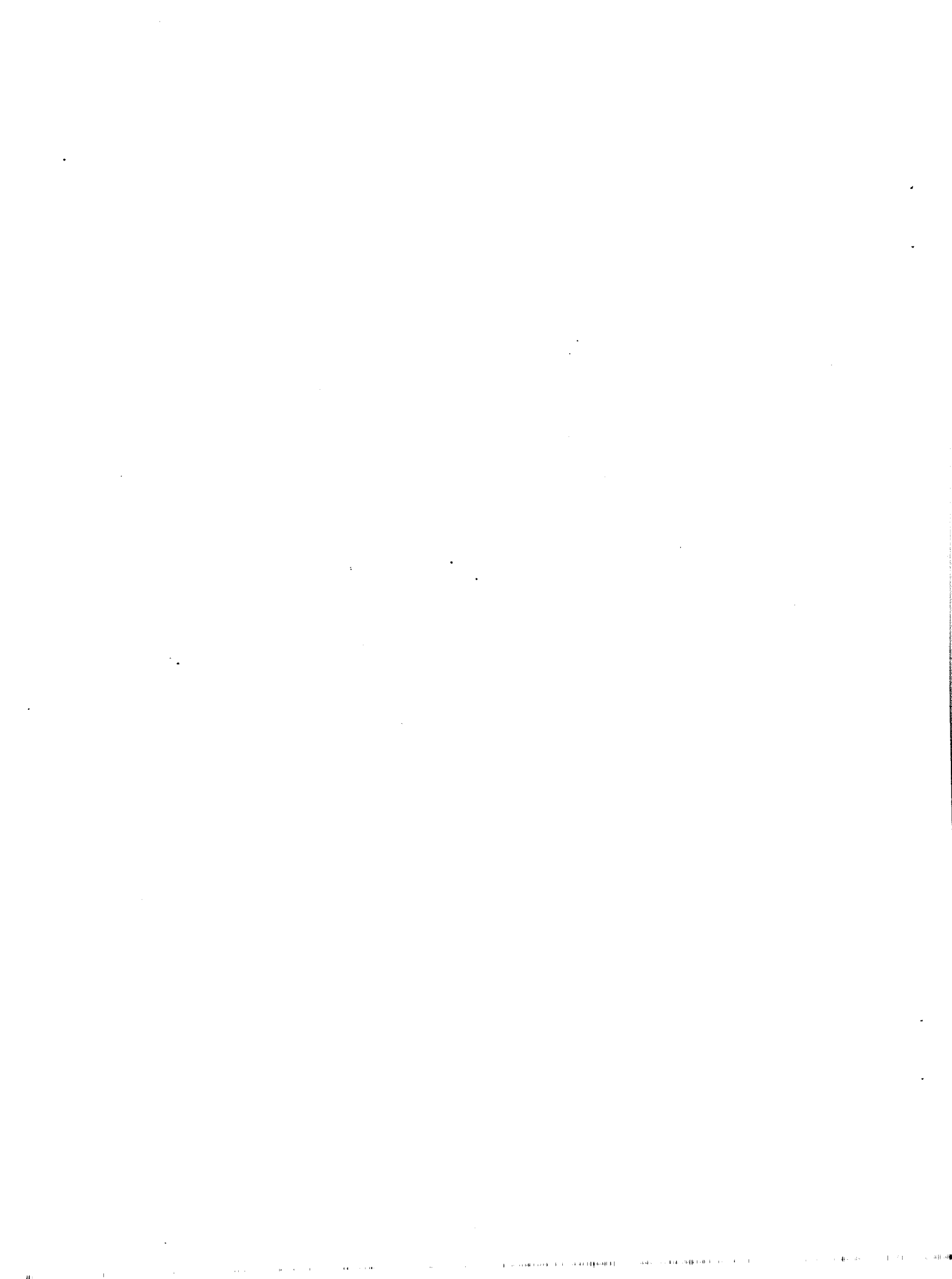
**NBS-GCR-86-515**

# **Spray Cooling in Room Fires**

**Hong-Zeng You, Hsiang-Cheng Kung,  
and Zhanxian Han**

**July 1986**

**Sponsored by  
U.S. DEPARTMENT OF COMMERCE  
National Bureau of Standards  
Center for Fire Research  
Gaithersburg, MD 20899**



NBS-GCR-86-515

**SPRAY COOLING IN ROOM FIRES**

Hong-Zeng You, Hsiang-Cheng Kung,  
and Zhanxian Han

Factory Mutual Research  
1151 Boston-Providence Turnpike  
Norwood, MA 02062

July 1986

NBS Grant Number NB83NADA4054

Sponsored by  
U.S. DEPARTMENT OF COMMERCE  
National Bureau of Standards  
Center for Fire Research  
Gaithersburg, MD 20899

### Notice

This report was prepared for the Center for Fire Research of the National Engineering Laboratory, National Bureau of Standards under Grant Number NB83NADA4054. The statements and conclusions contained in this report are those of the authors and do not necessarily reflect the views of the National Bureau of Standards or the Center for Fire Research.

TECHNICAL REPORT

SPRAY COOLING IN ROOM FIRES

by

Hong-Zeng You  
Hsiang-Cheng Kung  
Zhanxian Han\*

Prepared for  
United States Department of Commerce  
National Bureau of Standards  
Gaithersburg, MD 20899  
Under Grant No. NB83NADA4054

FMRC J. I. OJON9.RA  
070 (A)

March 1986

Approved by:

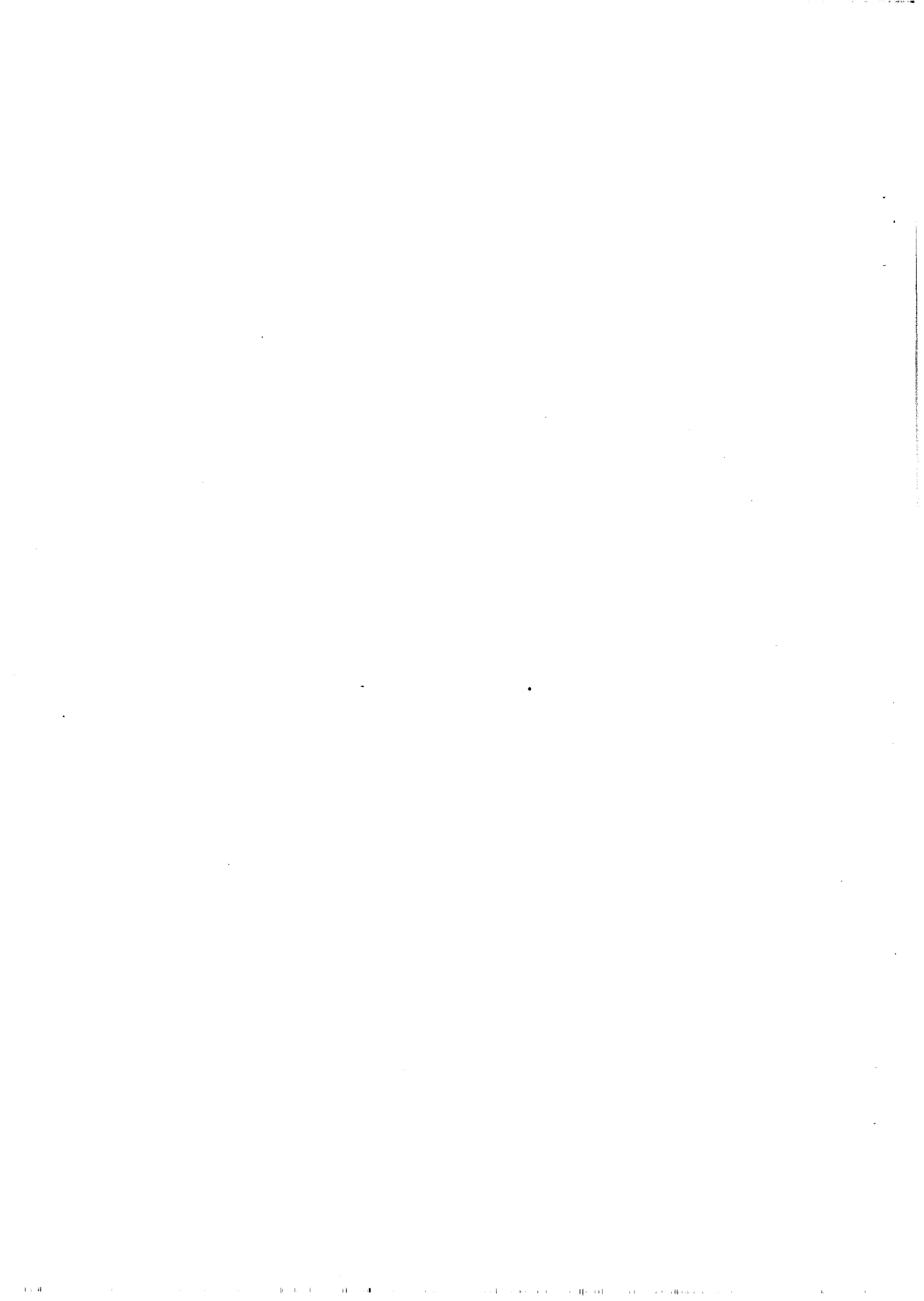
  
Cheng Yao  
Asst. Vice President & Manager  
Applied Research Department

\* Visiting scientist from Tianjin Fire Research Institute, Tianjin, China



**Factory Mutual Research**

1151 Boston-Providence Turnpike  
Norwood, Massachusetts 02062



FACTORY MUTUAL RESEARCH CORPORATION

OJON9.RA

ABSTRACT

A series of 25 fire tests was conducted to investigate cooling in room fires by sprinkler spray. The tests were conducted in a 3.66 m x 7.32 m x 2.44 m high test room, which had a 1.22 m x 2.44 m high opening centered in one of the 3.66 m walls. The fire source was a spray fire with constant heptane flow rate, located opposite the room opening. In each test only one sprinkler was installed at the ceiling. Three geometrically similar sprinklers with nozzle diameters of 11.1 mm, 8.36 mm, and 6.94 mm were tested.

Convective heat loss rate through the room opening was measured with a large fire products collector. The total heat release rate of the fire was derived from the fire products collector measurements using a carbon balance method. Heat loss rate to the ceiling and walls was measured, as well as radiative loss through the opening.

Empirical correlations for the heat absorption rate of the spray and the convective heat loss rate through the room opening were established in terms of 1) total heat release rate of the fire; 2) heat loss rate to the ceiling, walls, and floor, and radiative heat loss rate through the room opening; 3) room opening area and height; 4) sprinkler discharge rate; 5) water pressure; and 6) sprinkler orifice diameter. These correlations accounted for the effects of room geometry and opening size. Experimental results obtained for a different room geometry<sup>1</sup> also followed these correlations.

FACTORY MUTUAL RESEARCH CORPORATION

OJON9.RA

ACKNOWLEDGMENTS

The work was supported by the National Bureau of Standards, Department of Commerce, under Grant No. NB83NADA4054.

Messrs. W. R. Brown, E. E. Hill, and D. S. Mann constructed the test room and the fire products collector and set up instrumentation.

The valuable comments made by Mr. Edward K. Budnick of the National Bureau of Standards are sincerely appreciated.

FACTORY MUTUAL RESEARCH CORPORATION

OJON9.RA

TABLE OF CONTENTS

<u>Section</u>	<u>Title</u>	<u>Page</u>
ABSTRACT		i
ACKNOWLEDGMENTS		ii
I	INTRODUCTION	1
II	EXPERIMENTAL SETUP	3
	2.1 Test Room and Fire Products Collector	3
	2.2 Fire Source	3
	2.3 Sprinklers	7
	2.4 Instrumentation	7
III	DATA ANALYSIS AND RESULTS	13
	3.1 Energy Balance	13
	3.2 Spray Cooling	16
IV	CONCLUSIONS	21
NOMENCLATURE		22
REFERENCES		23
APPENDIX A	THE HOT-GAS-LAYER THICKNESS AT THE ROOM OPENING	25
APPENDIX B	THE VOLUMETRIC MEDIAN DROP SIZES OF WATER SPRAYS OF THREE GEOMETRICAL SIMILAR SPRINKLERS	31

FACTORY MUTUAL RESEARCH CORPORATION

OJON9.RA

LIST OF ILLUSTRATIONS

<u>Figure</u>	<u>Title</u>	<u>Page</u>
1	Plan View of the Test Room and Instrumentation Layout inside the Room Enclosure	4
2	The Fire Products Collector	5
3	The Fire Source	6
4	Detailed Dimensions of the 3/4-Scale Sprinkler a) Deflector and Supporting Rods	8
	b) Base and Orifice	9
5	Layout of Ten Surface Heat Flux Gages and Four Pairs of Surface Thermocouples	11
6	Correlation of Heat Absorption Rate of Sprinkler Spray	18
7	Correlation of Convective Heat Loss Rate through the Room Opening	19
A-1	Pressure Variations Inside and Outside the Room Opening	26
B-1	Locations of Drop Size and Water Flux Measurements	32
B-2	Correlation of Median Drop Size with Water Pressure and Sprinkler Nozzle Diameter	37

FACTORY MUTUAL RESEARCH CORPORATION

OJON9.RA

I

INTRODUCTION

Historically, water has been the most commonly used agent to suppress or extinguish fire. Means of delivering water to a fire by automatic sprinkler system was introduced about a century ago. Recently, sprinkler protection has gained considerable acceptance in health care facilities, hotels and residences. These occupancies are generally divided into rooms and hallways. As a fire develops in a room, combustion products generated from the fire tend to fill the room quickly due to the relatively low ceiling height and small room size. Radiation from the flame and hot ceiling gas layer may cause ignition of other combustibles in the room and may lead to fire flash-over eventually. Sufficient cooling of combustion products by sprinkler spray not only prevents ignition of other combustibles within the room, but also prevents fire spread and reduces smoke damage to adjacent rooms. Additionally, if the combustion gases are cooled sufficiently, actuation of sprinklers remote from the fire source can be prevented. Consequently, water demand for the sprinkler system will be small and the cost of the system will be affordable.

In an experimental study on spray cooling of hexane pool fires in a small room conducted by Kung<sup>1</sup>, the effects of fire size, sprinkler orifice diameter and water discharge pressure and water discharge rate on spray cooling ability were investigated. The test room was 3.05 m x 3.66 m x 2.44 m high. A pendent sprinkler was installed at the center of the ceiling. A hexane pool fire was located in the corner of the room, opposite the window opening. The heat absorption rate of the sprinkler spray was computed from an energy balance scheme. In the computation scheme, the heat release rate of the pool fire during sprinkler operation was based on the burning rate of the pool which was estimated from the weight loss history of the pool and the average rate of sprinkler water accumulation into the pool. The convective heat loss rate through the window opening was estimated from the temperature and velocity profiles at the opening. It was found that, for geometrically similar sprinklers, the heat absorption rate of sprinkler spray was directly proportional

## FACTORY MUTUAL RESEARCH CORPORATION

OJON9.RA

to the heat release rate and sprinkler discharge rate, and varied as the  $-0.73$  power of the volumetric median drop diameter\* of the spray.

Morgan and Baines<sup>2</sup> investigated heat transfer from a hot ceiling gas flow to a sprinkler spray for the case of a mall enclosure. The heat losses to the ceiling and walls of the mall were not measured directly, but obtained through an interpolation scheme based on the maximum temperature excess (above ambient) in the ceiling flow. A 1/2-in. diameter sprinkler was used for the test program. The investigation demonstrated that the sprinkler spray (at 99 to 123 l/min discharge rate) removed a significant amount of heat from the hot gas layer.

In this study, a large test room (3.66 m x 7.32 m x 2.44 m high) with a door opening opposite the fire source was used. The fire source was a heptane spray fire with constant heptane flow rate. Three of the five geometrically similar sprinklers previously used in Kung's study<sup>1</sup> were used. The effects of fire size, sprinkler water discharge rate and median drop diameter of sprinkler spray on the spray heat absorption rate and the convective heat loss rate through the room opening were investigated.

All the combustion products exiting from the test room opening were collected by a fire products collector, which was used to measure the convective heat loss rate through the room opening and the total heat release rate of the fire. With the fire products collector, such measurements could be performed accurately. Heat loss rate to the ceiling and walls was measured with heat flux gages and pairs of thermocouples; the radiative heat loss rate through the opening was measured with a radiometer. The heat loss rate to the floor was assumed to be mainly due to radiation from its fire source. Again, an energy balance scheme was used to compute the heat absorption rate of sprinkler spray. This heat absorption rate and the convective heat loss rate through the room opening were correlated with the test variables in a more general fashion than the correlation developed in Kung's study<sup>1</sup>, in order to account for the effects of room geometry and opening size. The correlations developed in this study have been applied successfully to Kung's data for a different room geometry and opening size. Such correlations should be useful to fire protection engineers in determining spray cooling ability.

---

\*The volumetric median diameter is defined as the diameter which divides the total volume of the spray drops into two equal parts; one part containing drops smaller than the median diameter, and the other part containing drops larger than the median diameter.

FACTORY MUTUAL RESEARCH CORPORATION

OJON9.RA

II

EXPERIMENTAL SETUP

2.1 TEST ROOM AND FIRE PRODUCTS COLLECTOR

The test room was built inside a large burn facility (12.2 m x 18.5 m x 10.1 m high). The test room itself was 3.66 m wide, 7.32 m long and 2.44 m high. A 1.22 m wide x 2.44 m high room opening was located at the center of the west wall, as shown in Figure 1. The test room was fabricated with "2 x 4" (1 1/2 in. x 3 3/8 in.) studs and "2 x 6" (1 1/2 in. x 5 1/4 in.) ceiling joists. The walls and ceiling were constructed with 13 mm thick plasterboards. Joint compound was used to seal the spaces between plasterboards.

A fire products collector was constructed over the room opening to collect the exiting combustion gases. The collector consisted of a 2.44-m diameter hood, a 0.61-m diameter stack, and other duct work (see Figure 2). An electric blower was installed in the duct work to exhaust combustion gases to the outside of the test facility. A 0.36-m diameter orifice plate was installed at the stack inlet to generate turbulence and achieve uniform flow inside the stack at the instrumentation station, about 3 m (five stack diameters) downstream of the orifice plate.<sup>3,4</sup>

2.2 FIRE SOURCE

The fire source was a heptane spray fire generated from a set of four oil-burner nozzles (Monarch). The four nozzles were mounted on a brass nozzle adaptor (Monarch) with nozzle axes parallel to one another. Heptane was supplied to the nozzle assembly (nozzles and adaptor) from a fuel tank through copper tubing. The fuel tank was pressurized with nitrogen gas. The copper tubing adjoining the nozzle assembly was cooled with a water jacket to maintain the fuel at a constant temperature. The nozzle assembly was shielded from direct sprinkler water impingement with a 3.1 mm thick steel plate, as shown in Figure 3. The fire source was located close to the east wall at equal distances from the north and south walls; the nozzle assembly and frame were positioned with respect to the east wall and the floor as shown in Figure 3.

ALL DIMENSIONS IN METERS

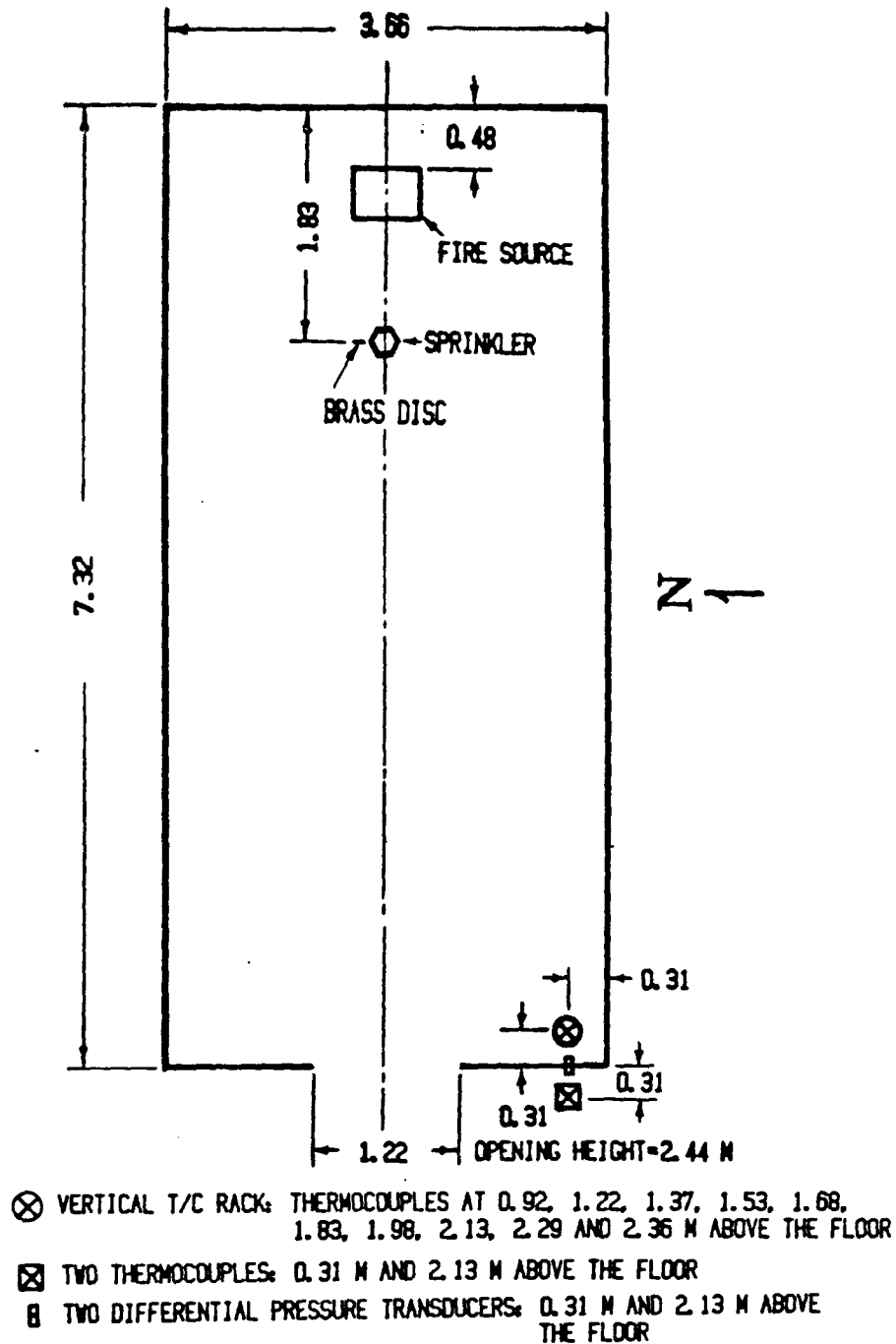


Figure 1 Plan View of the Test Room and Instrumentation Layout inside the Room Enclosure

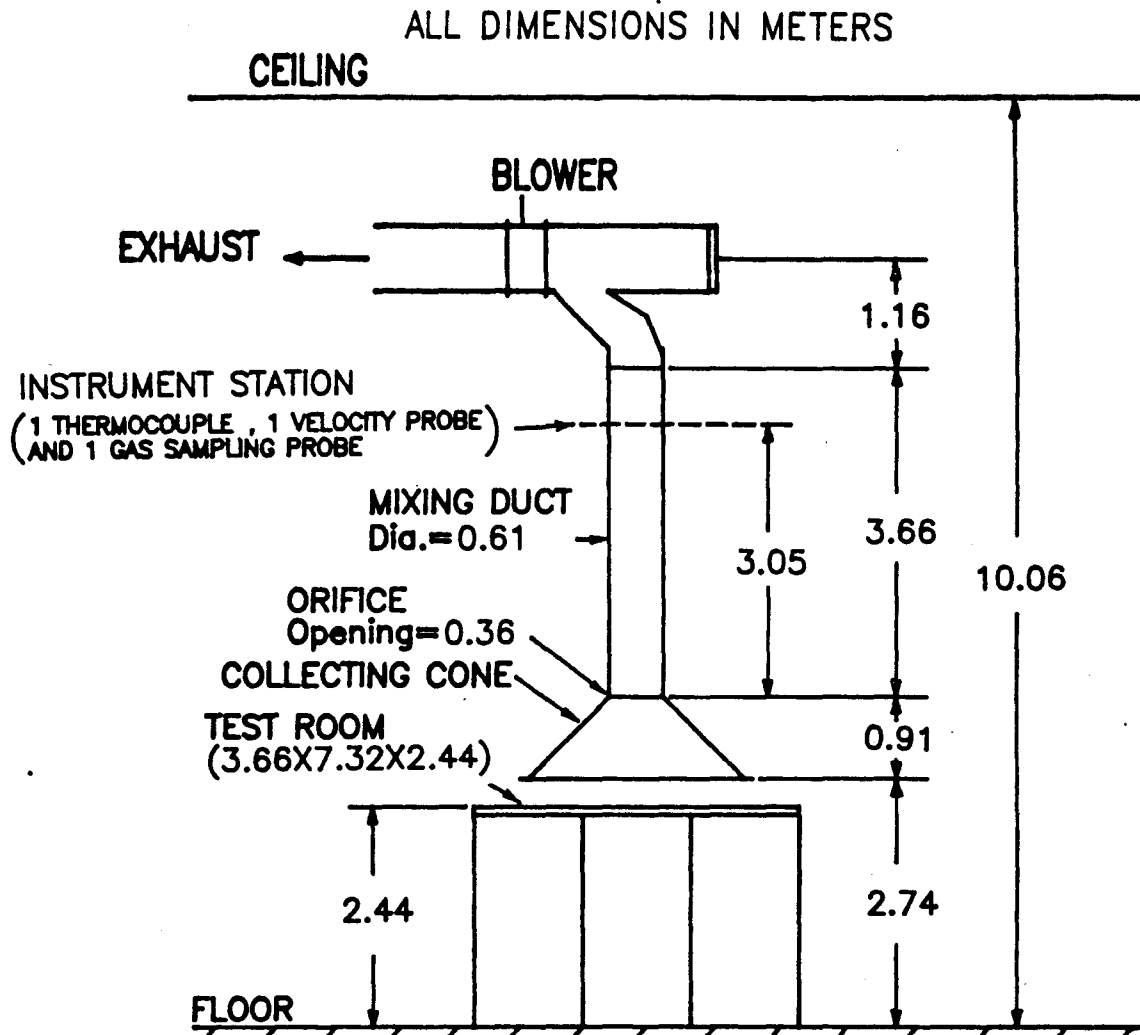


Figure 2 The Fire Products Collector

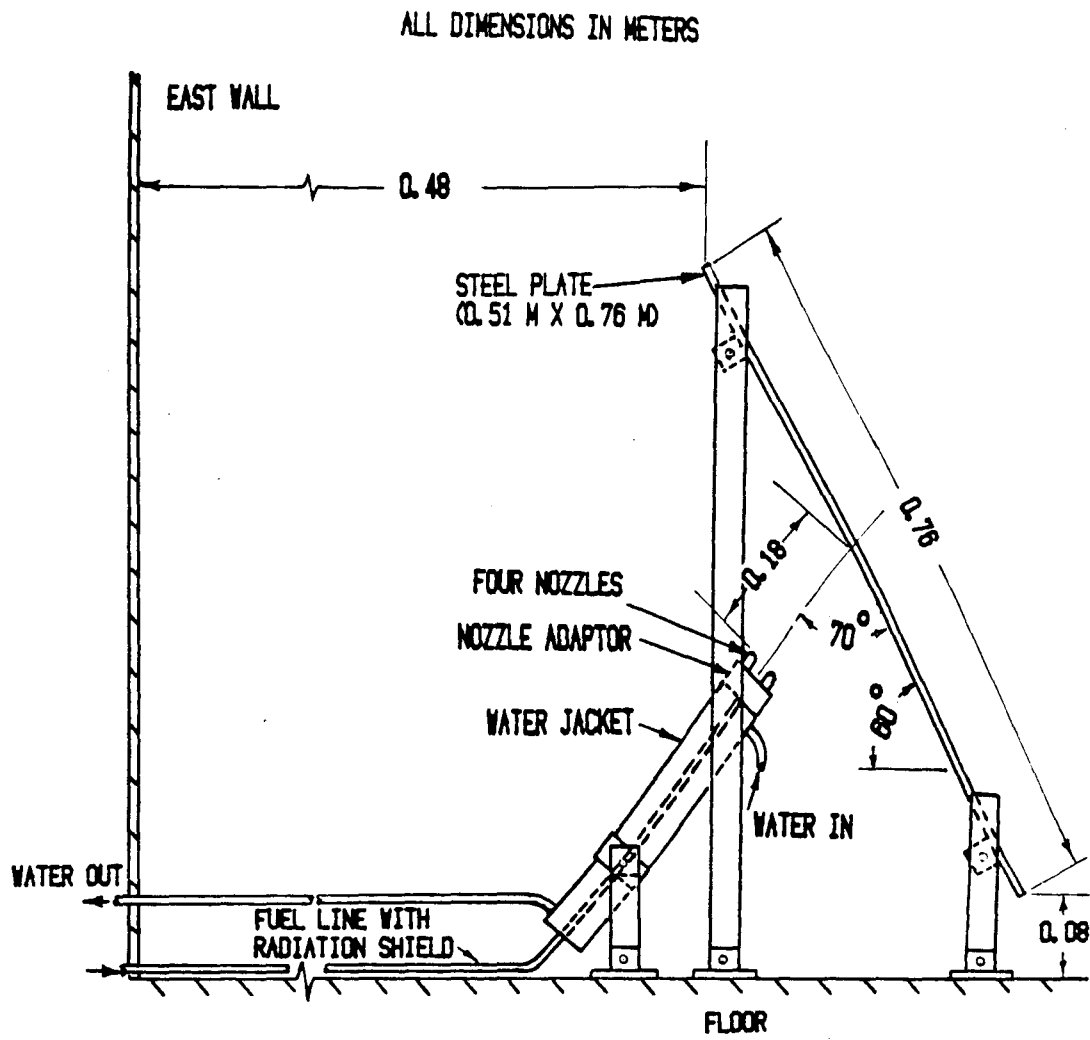


Figure 3 The Fire Source

## FACTORY MUTUAL RESEARCH CORPORATION

OJON9.RA

Three sets of nozzles of different capacity ratings (11.4, 15.1, and 18.9 l/hr of No. 2 fuel oil per nozzle at 690 kPa discharge pressure) were employed to obtain three heptane flow rates. Each nozzle produced a 70° solid cone spray at a discharge pressure of 690 kPa for No. 2 fuel oil.

### 2.3 SPRINKLERS

Three geometrically similar pendent sprinklers were used in this study. The orifice diameters of the three sprinklers were 11.1, 8.36 and 6.94 mm; the linear-scale ratios, referenced to the largest sprinkler, were 1, 3/4 and 5/8. Detailed dimensions of the 3/4-scale sprinkler nozzle are shown in Figure 4.

In each test, only one sprinkler was installed inside the test room equidistant from the north and south walls and 1.83 m from the east wall. The distance between the sprinkler deflector and the ceiling was 95 mm and the plane of the supporting rods for the deflector was parallel to the east wall.

The water flow to the sprinkler nozzle was controlled by a solenoid valve upstream of the nozzle. A simulated sprinkler link (brass disk) was installed in the vicinity of the sprinkler nozzle (50 mm from the nozzle centerline, 76 mm below the ceiling) to actuate the solenoid valve through a temperature controller when the link temperature reached 100°C above its initial temperature. The disk was constructed from brass shim stock, having a diameter of 25.4 mm and a thickness of 0.41 mm.

A flow meter and pressure gage were installed in the sprinkler piping system to measure sprinkler discharge rate and water pressure.

### 2.4 INSTRUMENTATION

The fire products collector was used to measure the total heat release rate of the fire and the convective heat loss rate through the room opening. The temperature, velocity and concentrations (CO, CO<sub>2</sub>, O<sub>2</sub> and total hydrocarbons) of the gases in the stack of the collector were measured at an instrumentation station located 3.05 m downstream of the collector orifice plate, where uniform flow of stack gases was achieved.

At the instrumentation station, a gas sampling port, a bidirectional pressure flow probe and a thermocouple were installed near the centerline of the collector stack (7 cm from the stack centerline). The gas sample was



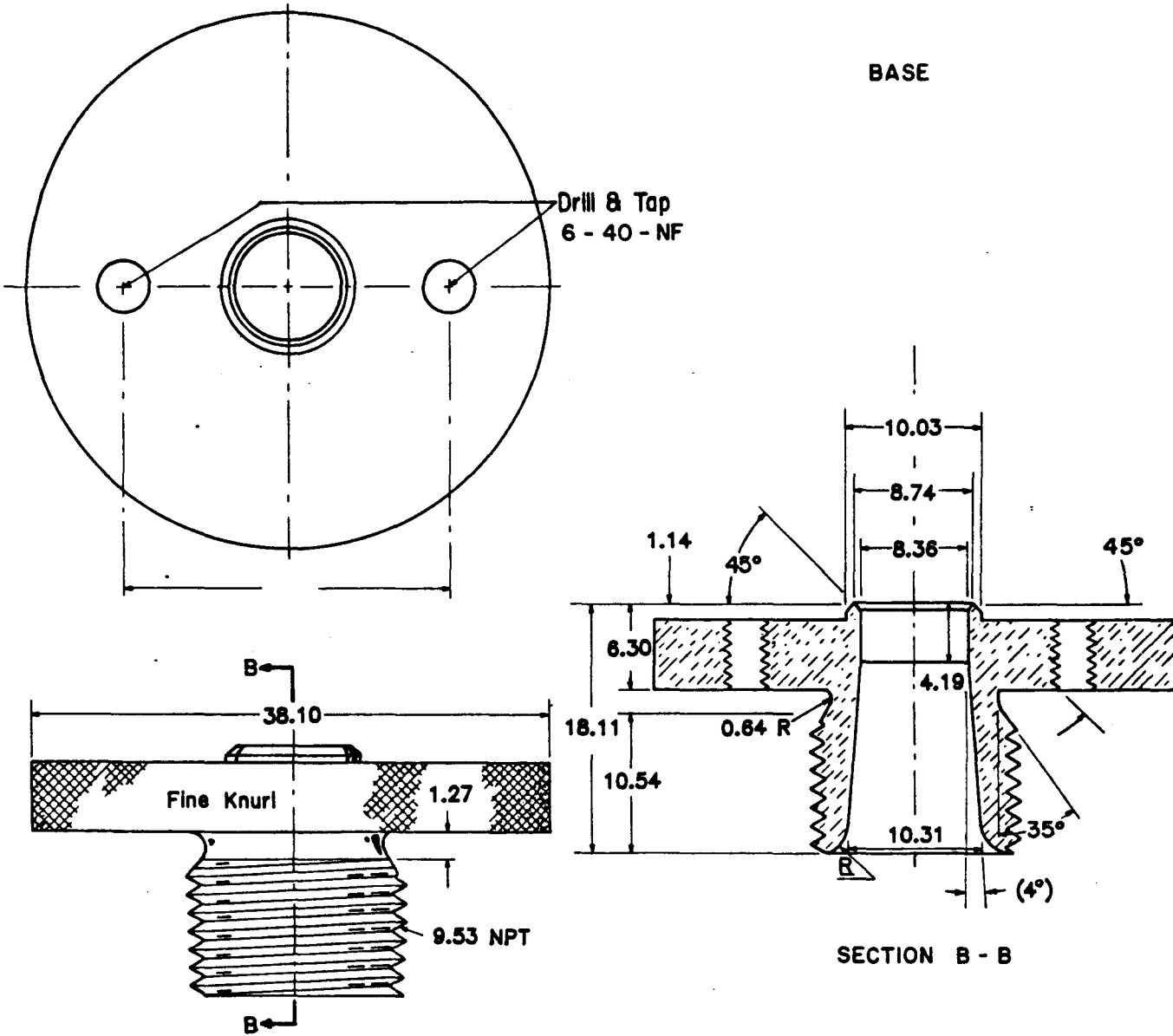


Figure 4 (Continued)

b) Base and Orifice

FACTORY MUTUAL RESEARCH CORPORATION

OJON9.RA

analyzed for concentrations of CO<sub>2</sub>, CO, O<sub>2</sub> and total hydrocarbons using Beckman Model 864 CO<sub>2</sub> Analyzer, Model 864 CO Analyzer, Model 755 O<sub>2</sub> Analyzer and Model 400 Hydrocarbon Analyzer, respectively. The flow probe was connected to an electronic manometer (Datametrics Model 1174 Barocel Electronic Manometer) to measure pressure differentials. The thermocouple was fabricated from 30 gage (0.25 mm diameter) inconel-sheathed, chromel-alumel thermocouple wire. Ambient gas temperatures inside the burn facility were monitored at five elevations (2.87 m, 4.39 m, 5.92 m, 7.44 m, and 8.97 m above the floor), near the west wall of the facility.

To determine the heat loss rate through the wall surfaces and the ceiling surface, surface heat flux gages (Model 20452-3 Micro-Foil, RdF Corp.) were installed on the ceiling and the walls and pairs of thermocouples on the inside and outside wall surfaces<sup>1</sup>. Since the gas flow and the sprinkler spray inside the room are expected to be symmetrical with respect to the east-west centerplane of the room, the heat loss rate through the wall and ceiling surfaces should also be symmetrical to the centerplane. Therefore, all the heat flux gages and surface thermocouples were installed on the ceiling and walls of the south half of the room. The locations of these instruments are shown in Figure 5.

To measure the radiative heat flux through the room opening, a radiometer (thermopile detector, Sensors, Inc., Type C-1) was placed outside the room in front of the opening, 1.22 m above the floor and 1.56 m from the opening. An adjustable rectangular opening was placed in front of the radiometer, so that the radiometer only viewed the room opening.

To determine the thickness of the ceiling hot gas layer at the room opening, we measured: 1) a vertical temperature traverse in the southwest corner of the room, 0.31 m from the south and the west walls, 2) ambient temperatures outside the room, close to the southwest corner at 2.13 m and 0.31 m above the floor, 3) pressure differences between the inside and outside of the room near the southwest corner at 2.13 and 0.31 m above the floor. The locations of these instruments are shown in Figure 1. All gas-temperature-measuring thermocouples were made of 30-gage inconel-sheathed, chromel-alumel thermocouple wire, having 0.37 mm diameter beads. Pressure differences were measured with electronic manometers (Datametrics Model 1173 Barocel Electronic Manometer). The methodology used to determine the ceiling hot gas thickness at the room opening from these measurements is provided in Appendix A.

ALL DIMENSIONS IN METERS

- ⊕ HEAT FLUX GAGE
- SURFACE THERMOCOUPLE PAIR ( INSIDE AND OUTSIDE )

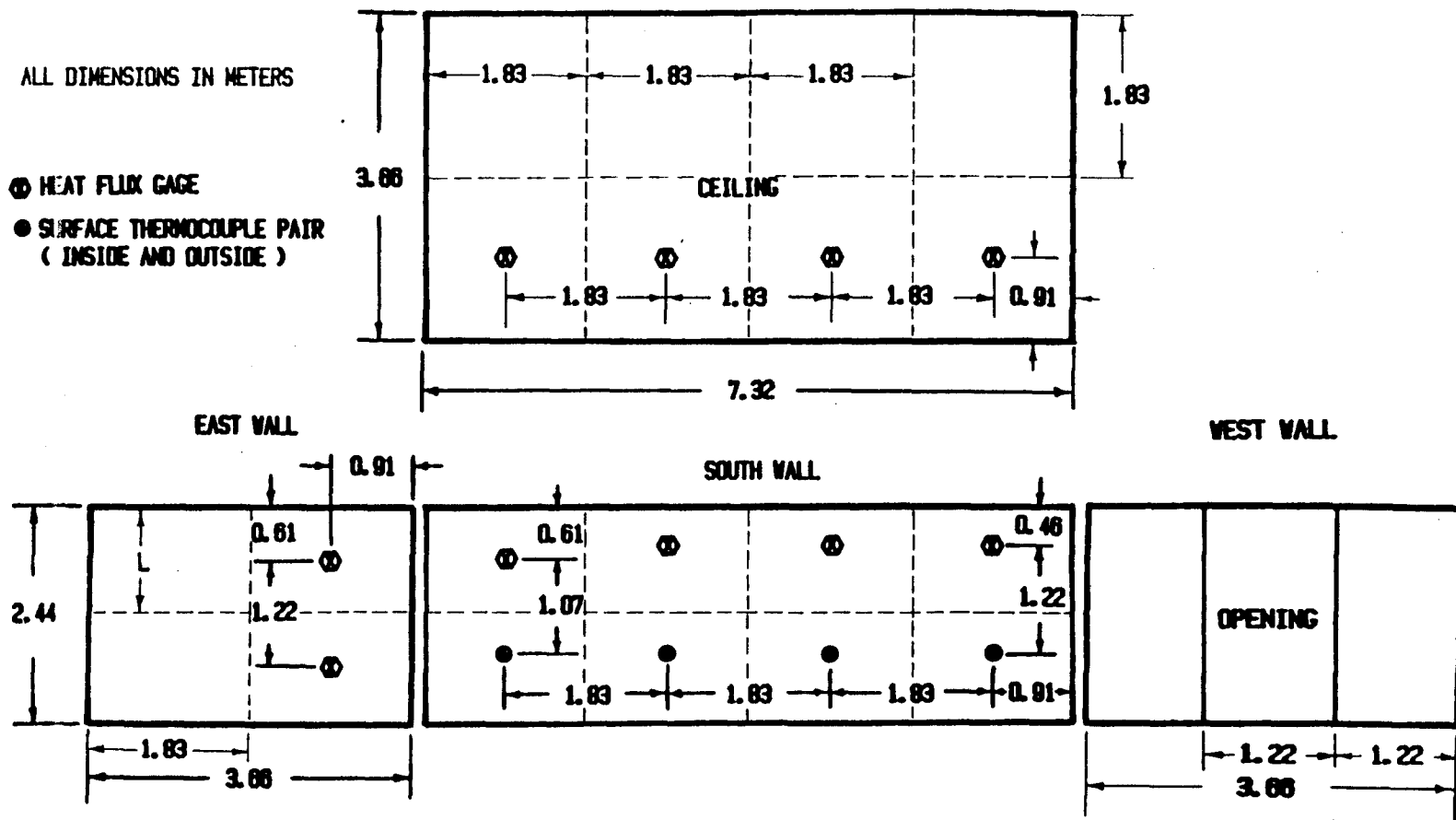


Figure 5 Layout of Ten Surface Heat Flux Gages and Four Pairs of Surface Thermocouples

FACTORY MUTUAL RESEARCH CORPORATION

OJON9.RA

All data signals were monitored by a data acquisition system with an HP 2100 A computer. Every 2 s the system scanned each data channel five times and logged the average values of five readings on a magnetic disk.

FACTORY MUTUAL RESEARCH CORPORATION

OJON9.RA

III

DATA ANALYSIS AND RESULTS

A series of 25 fire tests was conducted to investigate spray cooling in room fires. The major test variables included fire size, sprinkler orifice size, and water discharge rate. Table I presents a summary of the test conditions. For each test, the measurements used for analysis were taken within a period of 80 s after the gas phase inside the room reached a steady state. The beginning of the 80-s periods are tabulated in Table I.

3.1 ENERGY BALANCE

In the period of investigation, the energy balance equation pertaining to the entire volume inside the room enclosure is:

$$Q_a = Q_{cool} + Q_c + Q_\ell \quad (1)$$

where  $Q_a$  is the total heat release rate of the fire;  $Q_{cool}$  is the heat absorption rate of the sprinkler spray;  $Q_c$  is the convective heat loss rate through the room opening; and  $Q_\ell$  is the sum of the heat loss rate to the walls and ceiling ( $Q_g$ ), the heat loss rate to the floor ( $Q_f$ ) and the radiative heat loss rate through the opening ( $Q_r$ ).

The total heat release rate of the fire was determined from the measurements of gas concentrations and flow rate of the stack gases in the collector, using a carbon balance method. The method is based on the principle of mass conservation of elemental carbon involved in the combustion processes. For detailed description of the method, see Refs. 4 and 5.

The convective heat loss rate through the room opening,  $Q_c$ , was based on the measurements of gas temperature and flow rate of the stack gases in the collector, using  $Q_c = \dot{m} c_p \Delta T$ , where  $\dot{m}$ ,  $c_p$ , and  $\Delta T$  are the flow rate, specific heat and excess temperature (above ambient) of the stack gases, respectively. The gas temperature measured at 2.87 m above the floor near the west wall of the burn facility was used as the ambient temperature in the calculation. The specific heat of the stack gases was approximated by that of air<sup>6</sup>.

The heat loss rate to the south half of the walls and ceiling was assumed to equal that to the north half. The south wall and the south half of the

# FACTORY MUTUAL RESEARCH CORPORATION

OJON9.RA

ceiling and the east wall were divided into sections as shown in Figure 5. In each section a heat flux gage or a pair of thermocouples measured heat loss rate through the surface of the wall or ceiling. The height of the upper wall sections,  $L$ , was selected as the thickness of the ceiling gas layer at the room opening, which was determined from the vertical gas temperature profile and the pressure difference between the inside and outside near the southwest corner of the room (see Appendix A). Heat fluxes to the lower sections of the south wall were computed from the one-dimensional transient heat conduction equation using the measured inside and outside wall surface temperatures as boundary conditions. The thermal-property values of the wall used in the computation were heat capacity per unit of volume of the wall:  $818 \text{ kJ/m}^3\text{C}$  and thermal conductivity<sup>7</sup>:  $3.6 \times 10^{-4} \text{ kW/mC}$ . Since there was no heat flux gage or thermocouple pair on the west wall, the heat fluxes on the west wall surface were taken from the heat fluxes on the south wall at 0.91 m from the southwest corner. All heat flux values were averaged over the 80 s investigation period.

The radiative heat flux at the center of the room opening was derived from the radiometer measurement based on the assumption that the fire source emitted radiation isotropically from the center of the east wall. The radiative heat loss rate through the opening was the product of the radiative heat flux at the opening center and the room opening area.

The heat loss rate to the floor was assumed mainly due to radiation from the fire source. Isotropic heat radiation from the fire source was again assumed in order to estimate the radiative heat fluxes from the fire to the floor. The total heat loss rate to the floor area was then obtained by integrating the estimated radiative heat fluxes across the floor. It is obvious that the isotropy assumption would become invalid for the floor area close to the fire source. However, since the heat loss rate to the floor was only a small fraction of the total heat release rate of the fire (see Table I), the above isotropy assumption only introduced small errors in the energy balance results.

The various energy terms of the 25 fire tests are presented in Table I. The overall degree of accuracy of these terms was assessed by the results of the three freeburn tests: Tests 13, 17, and 21. Referring to the energy balance equation shown in Eq. (1), the difference between the lefthand side

FACTORY MUTUAL RESEARCH CORPORATION

OJON9.RA

TABLE I

ENERGY ITEMIZATION OF THE PRESENT TESTS

<u>Test No.</u>	<u>D</u> <u>(mm)</u>	<u>W</u> <u>(liter/min)</u>	<u>Begin-</u> <u>ning of</u> <u>Investi-</u> <u>gation</u> <u>Period (s)</u>	<u>Q<sub>a</sub></u> <u>(kW)</u>	<u>Q<sub>c</sub></u> <u>(kW)</u>	<u>Q<sub>r</sub></u> <u>(kW)</u>	<u>Q<sub>s</sub></u> <u>(kW)</u>	<u>Q<sub>f</sub></u> <u>(kW)</u>	<u>Q<sub>cool</sub></u> <u>(kW)</u>
1	6.94	45.4	360	150	24.0	0.1	18.4	4.4	103.1
2	6.94	68.2	360	148	4.6	< 0.1	16.0	2.6	124.7
3	6.94	45.4	360	314	65.0	0.2	30.3	10.6	207.9
4	6.94	68.9	360	306	22.8	< 0.1	26.8	3.7	252.6
5	6.94	45.4	360	494	122.0	0.3	48.1	15.0	308.6
6	6.94	68.2	360	486	58.0	0.1	38.0	4.9	385.0
7	8.36	40.1	390	149	53.6	0.1	20.9	6.0	68.4
8	8.36	68.2	360	140	15.1	< 0.1	16.7	3.5	104.6
9	8.36	45.4	360	304	101.1	0.2	33.7	12.6	156.4
10	8.36	68.2	400	316	57.4	< 0.2	30.5	7.7	220.2
11	8.36	45.4	363	447	162.6	0.5	55.6	24.8	203.5
12	8.36	68.2	360	472	104.3	0.2	42.4	11.8	313.3
13	11.10	0	310	134	91.0	0.3	31.0	13.0	0
14	11.10	45.4	360	135	73.0	0.1<	24.0	7.0	30.9
15	11.10	68.2	360	137	40.0	0.1	16.0	5.0	75.9
16	11.10	98.4	420	136	16.0	< 0.1	11.0	3.0	105.9
17	11.10	0	400	246	173.0	0.6	62.0	28.0	0
18	11.10	45.4	420	282	164.0	0.3	44.0	16.0	57.7
19	11.10	68.2	420	282	103.0	0.2	33.0	11.0	134.8
20	11.10	98.4	420	285	54.0	0.1	22.0	6.0	202.9
21	11.10	0	200	396	228.0	0.6	113.0	32.0	0
22	11.10	45.4	360	418	220.0	0.6	78.0	28.0	91.4
23	11.10	68.2	360	460	158.0	0.4	51.0	21.0	229.6
24	11.10	68.2	360	474	157.0	0.4	55.0	21.0	240.6
25	11.10	98.4	360	453	96.0	0.2	36.0	10.0	310.8

FACTORY MUTUAL RESEARCH CORPORATION

OJON9.RA

term and the sum of the righthand side terms is 1% of the total heat release rate for Test 13, 7% for Test 17, and 6% for Test 21.

3.2 SPRAY COOLING

The heat absorption rate of a sprinkler spray is expected to depend on the total surface area of the water drops,  $A_s$ , and the temperature of the ceiling gas layer in excess of the drop temperature,  $\Delta T$ . Since the water temperature was close to the ambient temperature,  $\Delta T$  could be taken as the excess temperature of the ceiling gas layer relative to the ambient temperature.

We may relate the total drop surface area,  $A_s$ , to sprinkler discharge rate,  $W$ , and the volumetric median drop size of the spray,  $d_m$ , by the formula:  $A_s \propto W/d_m$ . For geometrically similar sprinklers, the median drop size of the sprinkler spray was found<sup>8,9</sup> to be proportional to the  $-1/3$  power of water pressure,  $\Delta p$ , and  $2/3$  power of the sprinkler orifice diameter,  $D$ , i.e.,

$$A_s \propto (W^3 \Delta p D^{-2})^{1/3} \quad (2)$$

We performed drop size measurements of the sprinkler sprays tested in this program with the FMRC PMS drop-size measuring system<sup>10</sup>. Appendix B presents the measurements and drop size data of the sprinkler sprays. The data confirm the relationship represented by Eq. (2).

For freeburn room fires, the excess gas temperature of the ceiling gas layer can be expressed by<sup>11</sup>

$$\Delta T \sim Q_a^{2/3} (h_e A_e)^{-1/3} (A H^{1/2})^{-1/3} \quad (3)*$$

where  $h_e$  is the effective heat transfer coefficient from the gas phase inside the room to the room boundary;  $A_e$  is the effective room surface area;  $A$  and  $H$  are the area and height of the room opening<sup>11</sup>. Rearranging Eq. (3), we have:

$$\Delta T^{2/3} \sim Q_a^{2/3} (h_e A_e \Delta T)^{-1/3} (A H^{1/2})^{-1/3}$$

\*will break down if  $h_e \rightarrow 0$ .

FACTORY MUTUAL RESEARCH CORPORATION

OJON9.RA

or

$$\Delta T \sim Q_a Q_\ell^{-1/2} / (A H^{1/2})^{1/2} \quad (4)$$

where  $Q_\ell$  denotes the total heat loss rate to the room boundary, which is the sum of  $Q_r$ ,  $Q_s$ , and  $Q_f$ .

Combining Eqs. (2) and (4), we may postulate that the ratio of the heat absorption rate of the spray ( $\propto A_s \Delta T$ ) versus the total heat release rate of the fire,  $Q_{cool}/Q_a$ , is a function of  $\Lambda = (A H^{1/2} Q_\ell)^{-1/2} (W^3 \bar{\Delta p}^{-1} \bar{D}^{-2})^{1/3}$  where  $\bar{\Delta p} = \Delta p / (17.2 \text{ kPa})$  and  $\bar{D} = D / (0.0111 \text{ m})$ . Figure 6 presents a plot of  $Q_{cool}/Q_a$  versus  $\Lambda$ . It appears that the test data were well correlated in this form. The method of least squares was applied to fit the cooling rate data with the following formula:

$$Q_{cool}/Q_a = 0.000039 \Lambda^3 - 0.003 \Lambda^2 + 0.082 \Lambda \quad (5)$$

$$\text{for } 0 \leq \Lambda < 33 \text{ l}/(\text{min} \cdot \text{kW}^{1/2} \cdot \text{m}^{5/4}) .$$

For small values of  $\Lambda$ ,  $Q_{cool}/Q_a$  increased with  $\Lambda$  at a high rate, whereas for  $\Lambda > 20$ ,  $Q_{cool}/Q_a$  only increased moderately with  $\Lambda$ . The test data obtained by Kung for a different room geometry and opening size are also presented in Figure 6. Kung's data appeared to follow the same correlation as the data obtained in this study. The variable,  $\Lambda$ , in the present correlation has incorporated the effect of the room size through the heat loss rate to the room boundary,  $Q_\ell$ , and the effect of opening geometry through the ventilation factor  $A H^{1/2}$ .

The ratio of the convective heat loss rate versus the total heat release rate of the fire,  $Q_c/Q_a$ , is plotted against the variable,  $\Lambda$ , in Figure 7, which also includes Kung's data. The data obtained in this study and in Kung's study can be correlated successfully by the parameters developed. An empirical correlation between  $Q_c/Q_a$  and  $\Lambda$  is established as

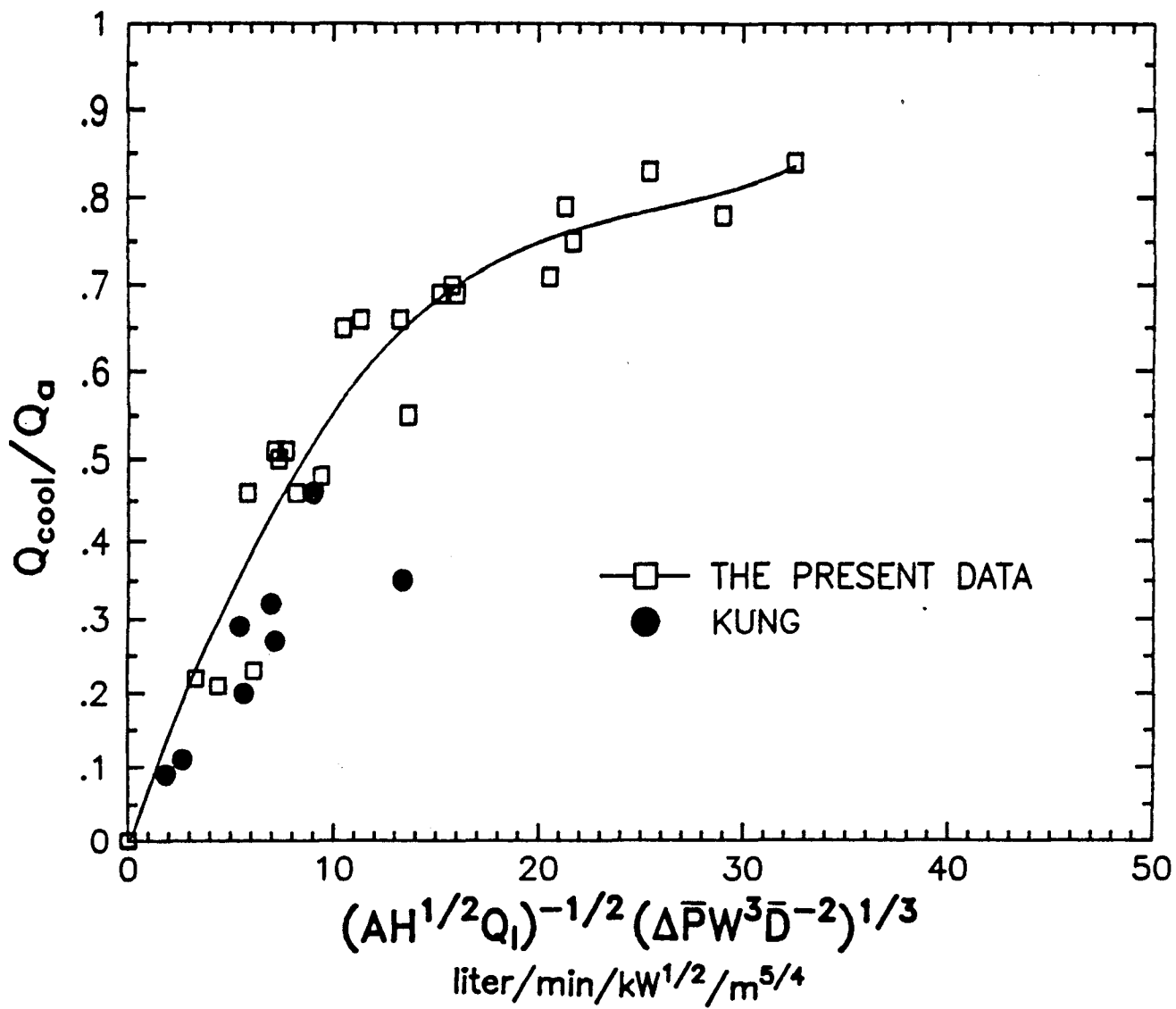


Figure 6 Correlation of Heat Absorption Rate of Sprinkler Spray

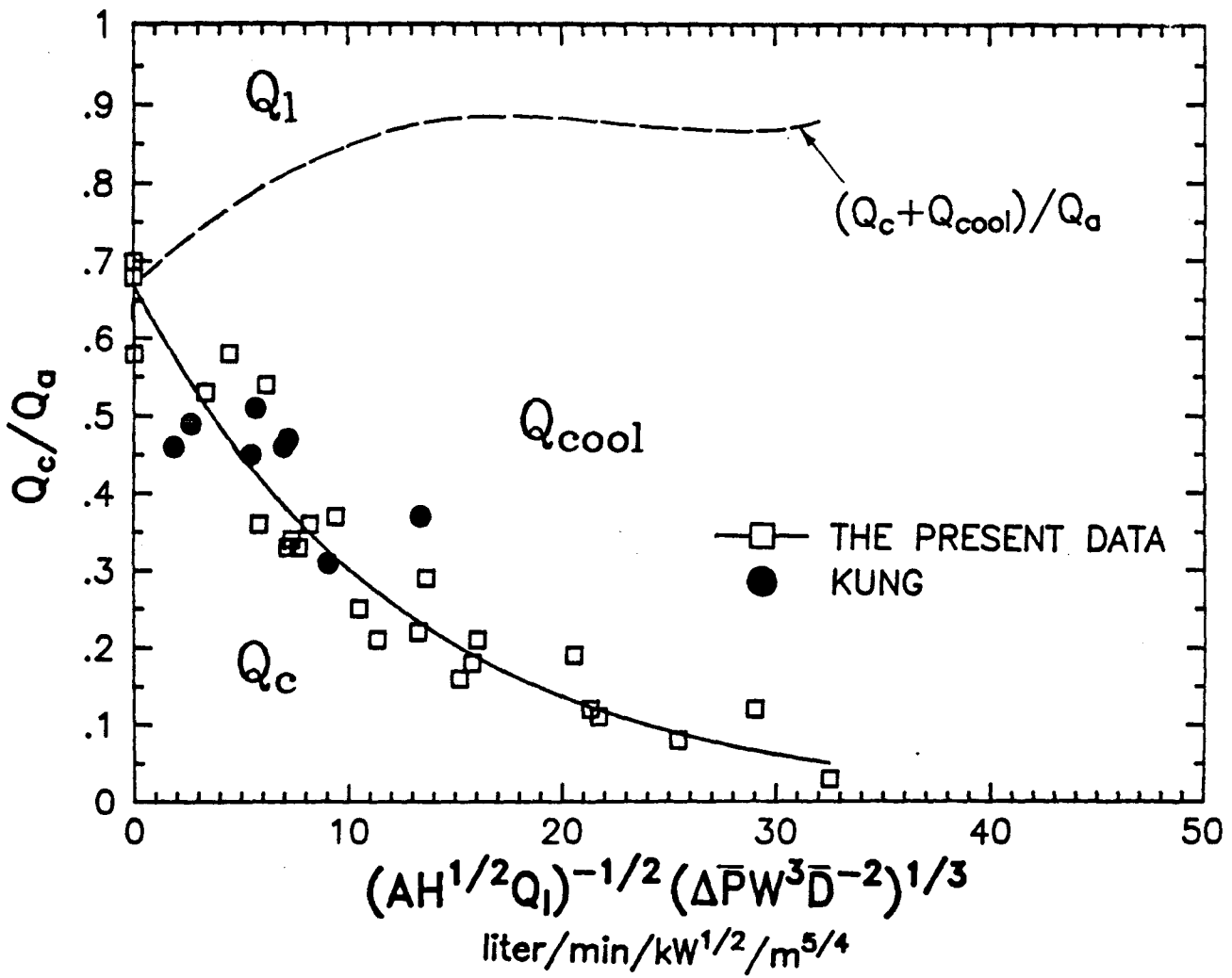


Figure 7 Correlation of Convective Heat Loss Rate through the Room Opening

OJON9.RA

$$Q_c/Q_a = 0.67 \exp(-0.08 \Lambda) \quad (6)$$

$$\text{for } 0 \leq \Lambda < 33 \text{ } \ell/(\text{min} \cdot \text{kW}^{1/2} \cdot \text{m}^{5/4}) .$$

A dashed curve representing the sum of  $Q_{\text{cool}}/Q_a$  (Eq. (5)) and  $Q_c/Q_a$  (Eq. (6)) is also shown in Figure 7. In the range of  $0 < \Lambda < 33 \text{ } \ell/(\text{min} \cdot \text{kW}^{1/2} \cdot \text{m}^{5/4})$ , the dashed curve and the solid curve divide the figure into three regions. From bottom to top, the regions correspond to the fractions of total heat release rate of fire convected out of the room opening,  $Q_c$ , absorbed by sprinkler spray,  $Q_{\text{cool}}$ , and lost to the room boundary,  $Q_\ell$ , respectively. As expected, less heat was convected through the opening as more heat was absorbed by the spray (larger value of  $\Lambda$ ).

The correlations developed above apply to room geometry with length-to-width ratio of 1.2-2 and opening size of 1.70-2.97 m<sup>2</sup>. For no-spray conditions, the ratio of convective heat loss rate through the room opening,  $Q_c$ , versus total heat release rate of the fire,  $Q_a$ , is about 0.58-0.7 in this study. However, we expect the ratio,  $Q_c/Q_a$ , would be different from the above values if the length-to-width ratio of a room is large, i.e., a long corridor.

FACTORY MUTUAL RESEARCH CORPORATION

OJON9.RA

IV

CONCLUSIONS

Empirical correlations for the heat absorption rate of sprinkler spray in a room fire and the convective heat loss rate through a room opening were established from the data obtained in this study in terms of 1) the total heat release rate of the fire; 2) the sum of the heat loss rate to the ceiling, walls, and floor and the radiative heat loss rate through the room opening; 3) room opening area and height; 4) sprinkler discharge rate; 5) water pressure; and 6) sprinkler orifice diameter.

These correlations are more general than Kung's correlation<sup>1</sup>, in which only the variables concerning sprinkler spray characteristics and fire size were considered; however, the present correlations account for the effects of room geometry and opening size, in addition to the spray characteristics and fire size. These correlations were applied successfully to Kung's previous data for a different room size, opening size, and fire source.

NOMENCLATURE

A	room opening area ( $m^2$ )
$A_s$	total surface area of water drops ( $m^2$ )
$A_e$	effective room surface area for heat transfer ( $m^2$ )
$C_p$	specific heat of air ( $kJ/kg \cdot C$ )
D	sprinkler nozzle diameter (m)
H	room opening height (m)
$h_e$	effective heat transfer coefficient from gas phase inside the room to the room boundary ( $kW/m^2 \cdot C$ )
$\dot{m}$	gas flow rate in the fire products collector (kg/s)
$\Delta p$	water pressure (kPa)
$Q_a$	total heat release rate of the fire (kW)
$Q_c$	convective heat loss rate through the room opening (kW)
$Q_{cool}$	heat absorption rate of sprinkler spray (kW)
$Q_f$	heat loss rate to the room floor (kW)
$Q_\ell$	the sum of $Q_f$ , $Q_s$ and $Q_r$ (kW)
$Q_r$	radiative heat loss rate through the room opening (kW)
$Q_s$	heat loss rate to the walls and ceiling (kW)
$\Delta T$	excess temperature (above ambient) of stack gases, or excess temperature of the hot gas layer inside the room (C)
W	sprinkler water discharge rate (liters/min)

FACTORY MUTUAL RESEARCH CORPORATION

OJON9.RA

REFERENCES

- 1) Kung, H.C.: "Cooling of Room Fires by Sprinkler Spray," ASME Journal of Heat Transfer, 99, p. 353, August 1977.
- 2) Morgan, H.P. and Baines, K.: "Heat Transfer from a Buoyant Smoke Layer Beneath a Ceiling to a Sprinkler Spray, Part 2 - An Experiment," Fire and Materials, 3, 1, p. 34, 1979.
- 3) Ebaugh, N.C. and Whitfield, R.: "The Intake Orifice and a Proposed Method for Testing Exhaust Fans," Transaction of ASME, 56, p. 903, 1934.
- 4) Heskestad, G.: "A Fire Products Collector for Calorimetry into the MW Range," FMRC Technical Report, J.I. OC2E1.RA, Factory Mutual Research Corporation, Norwood, Massachusetts, June, 1981.
- 5) Tewarson, A.: "Flame-Retarded Polymeric Materials - Vol. 3", p. 97, edited by Lewin, M., Atlas, S.M. and Pearce, E.M., Plenum Press, New York, 1982.
- 6) Holman, J.P.: Heat Transfer, McGraw-Hill, Inc., New York, 1976.
- 7) Croce, P.A.: "Energy Balance for the Bedroom Enclosure," The Third Full-Scale Bedroom Fire Test of the Home Fire Project (July 30, 1975), Vol. II - Analysis of Test Result, edited by A.T. Modak, FMRC Technical Report, No. 210117, the Factory Mutual Research Corporation, Norwood, Massachusetts, 1976.
- 8) Heskestad, G.: "Proposal for Studying Interaction of Water Sprays with Plume in Sprinkler Optimization Program," FMRC Interoffice Correspondence, 1972.
- 9) Dundas, P.H.: "Optimization of Sprinkler Fire Protection, Progress Report No. 10, the Scaling of Sprinkler Discharge: Prediction of Drop Size," FMRC Technical Report, No. 18792, the Factory Mutual Research Corporation, Norwood, Massachusetts, 1974.
- 10) You, H.Z. and Symonds, A.P.: "Sprinkler Drop-Size Measurement, Part I: An Investigation of the FMRC PMS Drop-Size Measuring System," FMRC Technical Report J.I. OG1E7.RA, Factory Mutual Research Corporation, Norwood, Massachusetts, December 1982.
- 11) McCaffrey, B.J., Quintiere, J.G., and Harkleroad, M.F.: "Estimating Room Temperatures and the Likelihood of Flashover Using Fire Test Data Conditions," Fire Technology, 17, p. 98, 1981.

FACTORY MUTUAL RESEARCH CORPORATION

OJON9.RA

- 12) Quintiere, J.G. and DenBraven, K.: "Some Theoretical Aspects of Fire Induced Flows through Doorways in a Room-Corridor Scale Model," Center for Fire Research Report No. NBSIR-78-1512, National Bureau of Standards, U.S. Department of Commerce, October, 1978.

OJON9.RA

## APPENDIX A

THE HOT-GAS-LAYER THICKNESS AT THE ROOM OPENING

The thickness of the hot gas layer at the room opening is defined as the distance between the ceiling and the "neutral plane." The neutral plane is a gas layer boundary above which the hot gas leaves the room and below which cold ambient air enters the room. The methodology to determine the neutral plane location from the vertical gas temperature profile and the pressure difference between the inside and outside near the opening was developed by Quintiere and DenBraven<sup>12</sup>.

Since the mean gas velocity at the neutral plane is zero, the stagnation pressure inside the room balances the outside ambient pressure at the level of the neutral plane. Figure A-1 schematically depicts the gas flows and the vertical variations of stagnation pressure inside and outside the room. In the figure,  $H$ ,  $Z_n$ , and  $Z_t$  denote the distances measured from the floor to the ceiling, to the neutral plane, and to the elevation of discontinuity of gas temperature inside the room.

Referring to Figure A-1, the difference between the pressures inside and outside the room opening at the elevation of  $y_1$  above the neutral plane is

$$\Delta P_{io1} = \int_0^{y_1} (\rho_o - \rho_i) g dy \quad (A.1)$$

where  $\rho_o$  and  $\rho_i$  denote the gas density outside and inside the room, respectively.

Similarly, the pressure difference at the elevation of  $y_2$  above the neutral plane is

$$\Delta P_{io2} = \int_0^{y_2} (\rho_o - \rho_i) g dy . \quad (A.2)$$

Therefore

$$\Delta P_{io2} = \Delta P_{io1} + \int_{y_1}^{y_2} (\rho_o - \rho_i) g dy . \quad (A.3)$$

For the tests conducted in this study, the variation of ambient temperature from the floor level to the ceiling level was small. Therefore, for each

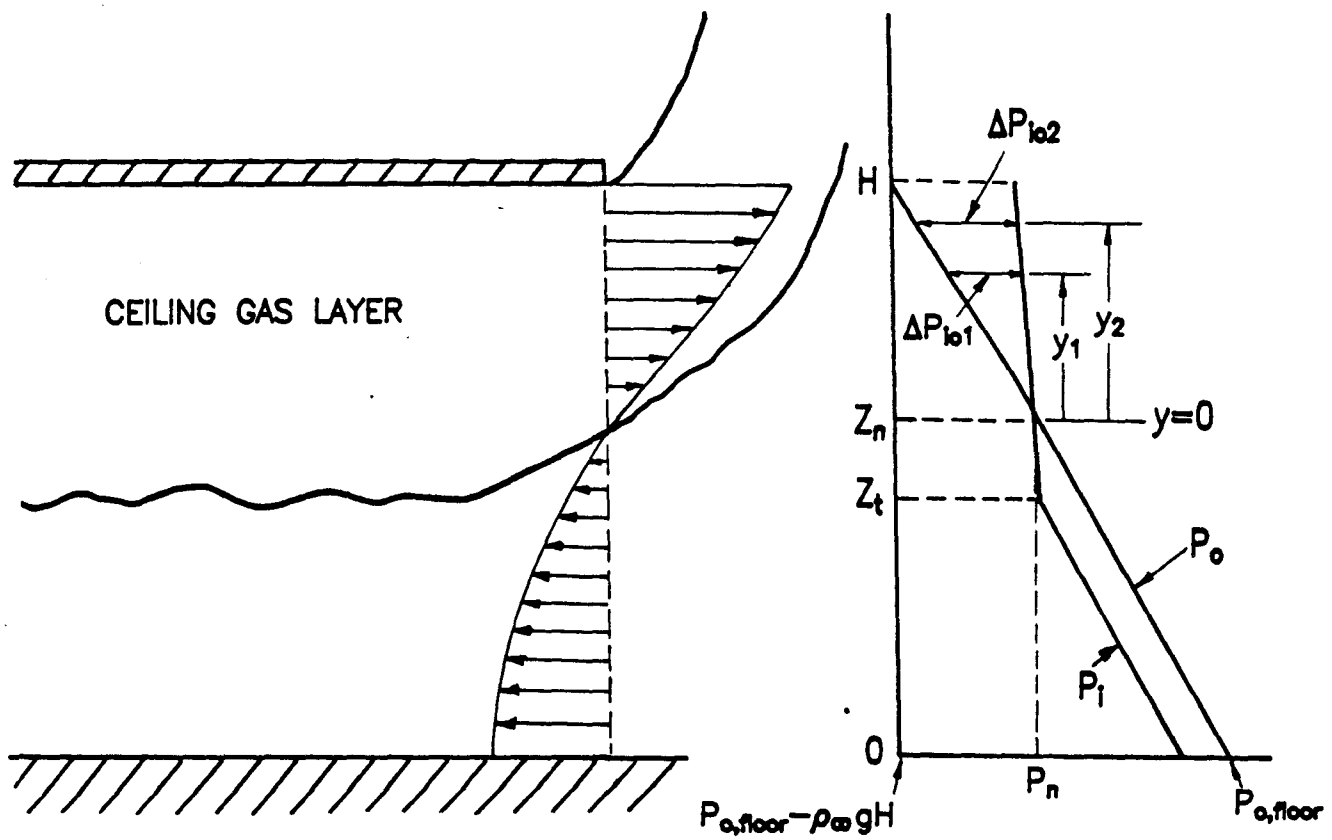


Figure A-1 Pressure Variations Inside and Outside the Room Opening

OJON9.RA

test,  $\rho_0$  can be replaced by the ambient density,  $\rho_\infty$ , which is constant from the floor level to the ceiling level.

Equation (A.3) thus becomes:

$$\Delta P_{io2} = \Delta P_{io1} + \rho_\infty g \int_{y_1}^{y_2} \frac{\Delta T}{T_i} dy . \quad (A.4)$$

If  $\Delta T_{io1}$  and  $\Delta T_{io2}$  represent the temperature differences at level  $y_1$  and level  $y_2$  respectively, the temperature differences between  $y_1$  and  $y_2$  may be linearly interpolated from  $\Delta T_{io1}$  and  $\Delta T_{io2}$  by

$$\Delta T = \Delta T_{io1} + (\Delta T_{io2} - \Delta T_{io1}) (y - y_1)/(y_2 - y_1) . \quad (A.5)$$

Substituting Eq. (A.5) into Eq. (A.4) and letting  $C_t = \Delta T_{io2} - \Delta T_{io1}$  and  $\ell = y_2 - y_1$ , we obtain

$$\begin{aligned} \Delta P_{io2} &= \Delta P_{io1} + \rho_\infty g \int_{y_1}^{y_2} \frac{\Delta T_{io1} + C_t (y - y_1)/\ell}{T_{i1} + C_t (y - y_1)/\ell} dy \\ &= \Delta P_{io1} + \rho_\infty g \ell \int_0^1 \frac{\Delta T_{io1} + C_t y'}{T_{i1} + C_t y'} dy' \\ &= \Delta P_{io1} + \rho_\infty g \ell \left[ 1 + \frac{T_\infty}{C_t} \ln (T_{i1}/T_{i2}) \right] \end{aligned} \quad (A.6)$$

where  $y' = (y - y_1)/\ell$ .

The location of the neutral plane corresponds to the level where  $\Delta P_{io1} = 0$ . Based on Eq. (A.6)

$$\Delta P_{io2} = \sum_m \rho_\infty g \ell_m \left[ 1 + (T_\infty/C_{t,m}) \ln (T_{i1,m}/T_{i2,m}) \right] \quad (A.7)$$

at the neutral plane. In Eq. (A.7),  $\Delta P_{io2}$  is the pressure difference measured at level  $y_2$  and  $m$  denotes that there are  $m$  intervals between temperature measurements from the level  $y_2$  to the neutral plane.

In this study, the location of the neutral plane was determined based on temperature measurements of the corner thermocouple rack located 31 cm from the south wall and 31 cm from the west wall together with the measurement of

FACTORY MUTUAL RESEARCH CORPORATION

OJON9.RA

hydrostatic pressure difference,  $\Delta P_{i02}$ , on the west wall 31 cm below the ceiling. Table A.1 presents the distances from the ceiling to the neutral plane for the 25 fire tests.

FACTORY MUTUAL RESEARCH CORPORATION

OJON9.RA

TABLE A.1

HOT-GAS-LAYER THICKNESS AT THE ROOM OPENING

<u>Test No. *</u>	<u>Hot-Gas-Layer Thickness (m)</u>
1	0.76
2	0.76
3	1.00
4	0.91
5	1.07
6	0.96
7	0.92
8	0.80
9	1.05
10	0.94
11	1.07
12	1.05
13	0.87
14	0.98
15	1.12
16	0.91
17	1.05
18	1.07
19	1.03
20	1.08
21	1.05
22	1.18
23	1.18
24	1.24
25	1.22

\* Refer to Table I for test variables



OJON9.RA

## APPENDIX B

THE VOLUMETRIC MEDIAN DROP SIZES OF WATER SPRAYS OF  
THREE GEOMETRICAL SIMILAR SPRINKLERS

Seven different sprinkler sprays were tested for their ability to cool room fires. Three geometrically similar pendent sprinklers, the same as those used in Kung's spray cooling study<sup>1</sup>, were employed to provide these seven sprays. Table B.1 lists the water pressures, water discharge rates, and sprinkler nozzle diameters for these sprays.

## B.1 SETUP AND PROCEDURE

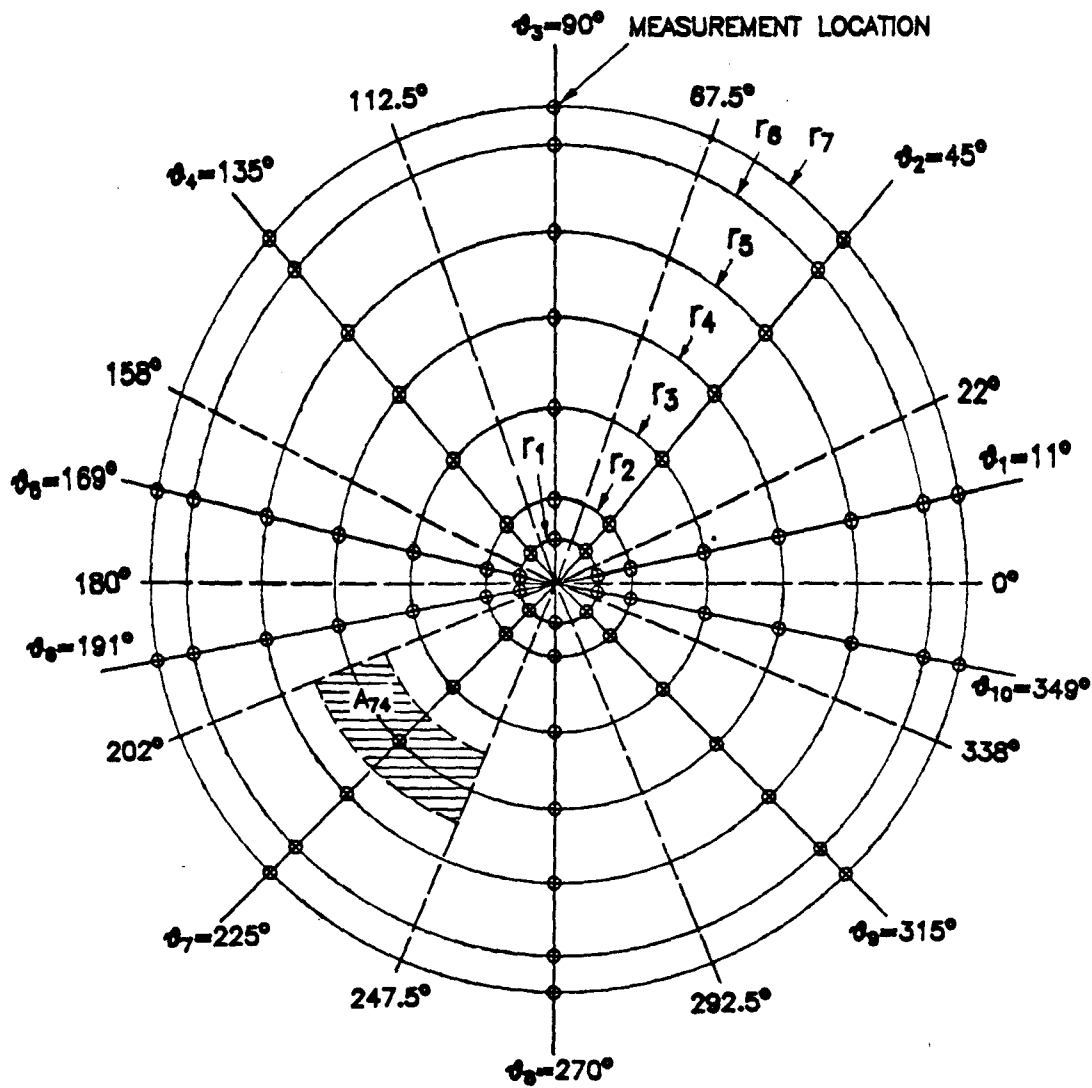
All the drop size and water flux measurements were made in the FMRC Hydraulics Laboratory. Drop sizes were measured with the FMRC PMS drop-size measuring system<sup>10</sup>; water fluxes were measured with 30.5-cm x 30.5-cm x 61.0-cm high pans.

The sprinkler was centered underneath a 6.10-m x 7.62-m suspended ceiling, which was 3.30 m above the floor. The distance between the ceiling and the sprinkler base was 58 mm. The sprinkler was connected to a nominal 1/2 in. steel pipe (0.3-m long).

For each sprinkler spray, distributions of water flux and drop size were mapped out in a horizontal cross section 2.08 m below the ceiling. Figure B-1 illustrates the measurement locations in this horizontal cross section. The two supporting rods of each sprinkler were aligned with radii of 0 and 180 degrees. A bench, capable of sweeping azimuthally 360° across the spray, was used to traverse the drop size measuring probe or the water-flux measuring pans to the azimuthal positions shown in Figure B-1. One end of the bench was pivoted on the floor and directly under the sprinkler (the coordinate origin).

A pressure tap was provided upstream of the sprinkler for monitoring the water pressure. A float area meter was used to measure the water discharge rate.

For drop size measurements, the averaged sample size of water drops was about 2000 drop counts in a 3-min period at locations 0.61 m from the spray centerline; the averaged sample size was about 300 counts in a 6-min period at measuring locations along the spray perimeter. For water flux measurements, the period of the water collection was 10 min.



\* The radial distances of  $r_1$  to  $r_7$  are 0.31 m, 0.61 m, 1.22 m, 1.83 m, 2.44 m, 3.05 m and 3.35 m, respectively.

Figure B-1 Locations of Drop Size and Water Flux Measurements

OJON9.RA

## B.2 RESULTS

The gross drop size distribution of a spray at 2.08 m below the ceiling was estimated from the measurements of local drop size distribution and water flux at locations shown in Figure B-1 through the following two equations:

$$APV_{\ell} = \frac{\sum_{p=1}^P \sum_{i=1}^I A_{ip} \dot{V}_{ip}''}{W} APV_{ip\ell} \quad (B.1)$$

and

$$W = \sum_{p=1}^P \sum_{i=1}^I A_{ip} \dot{V}_{ip}'' \quad (B.2)$$

In these equations,  $APV_{ip\ell}$  is the local accumulative percent of water volume below a drop size,  $d_{\ell}$ , at the location,  $ip$ , specified by the  $i$ -th azimuthal angle and the  $p$ -th radial distance;  $A_{ip}$  and  $\dot{V}_{ip}''$  are the designated surface area and water flux of the horizontal area which contains the location,  $ip$  (see Figure B-1). It was assumed that the measurements of local drop size distribution and water flux in an area,  $A_{ip}$ , represented the corresponding averaged values in the entire area,  $A_{ip}$ .

The horizontal cross section of the spray 2.08 m below the ceiling was divided into a number of  $A_{ip}$ 's; each  $A_{ip}$  contained a measuring location. Each  $A_{ip}$  was delimited by 1) two concentric arcs, one with a shorter radius,  $r_p - \frac{1}{2}$ , and the other with a longer radius,  $r_p + \frac{1}{2}$ , and 2) two radii. All the delimiting radii are shown in broken lines in Figure B-1. Except for the outermost areas ( $A_{ip}$ 's along the spray perimeter) and the innermost areas (surrounding the spray center),  $r_p - \frac{1}{2}$  was the average of  $r_p$  and  $r_{p-1}$ , and  $r_p + \frac{1}{2}$  was the average of  $r_p$  and  $r_{p+1}$ . For the outermost  $A_{ip}$ 's,  $r_p + \frac{1}{2}$  was determined to be the radial distance at the outer edge of the water collecting pan. For the innermost  $A_{ip}$ 's,  $r_p - \frac{1}{2}$  was assigned a value of zero.

Based on the data reduction method described, the gross drop size distributions of the seven sprays defined in Table B.1 were calculated. The volumetric median drop size of each spray could then be easily determined. The volumetric median drop size,  $d_m$ , is a characteristic drop size below which

FACTORY MUTUAL RESEARCH CORPORATION

OJON9.RA

TABLE B.1  
SPRAY VARIABLES

<u>Spray</u>	<u>Water Pressure (kPa)</u>	<u>Water Discharge Rate (liters/min)</u>	<u>Nozzle Diameter (mm)</u>
1	278	45.4	6.94
2	593	68.1	6.94
3	152	45.4	8.36
4	288	68.1	8.36
5	75	45.4	11.10
6	133	68.1	11.10
7	233	98.4	11.10

FACTORY MUTUAL RESEARCH CORPORATION

OJON9.RA

the accumulative percent of water volume (APV) is 50%. Table B.2 tabulates the volumetric median drop sizes and associated water discharge rates calculated by Eq. (B.2) for the sprays. The calculated water discharge rates are generally in good agreement with the corresponding actual water discharge rates (within 10%) except for the cases of  $D = 6.94$  mm and  $\Delta P = 278$  kPa, and  $D = 11.1$  mm and  $\Delta P = 233$  kPa. The discrepancy is 12.5% for the former and about 20% for the latter.

B.3 RELATIONSHIP BETWEEN VOLUMETRIC MEDIAN DROP SIZE AND WATER PRESSURE AND SPRINKLER NOZZLE DIAMETER

For geometrically similar nozzles, Heskestad found that at room temperature, the characteristic drop size can be related to the orifice size,  $D$ , and water pressure,  $\Delta P$ , by the following expression<sup>8</sup>:

$$d_m \sim \Delta P^{-1/3} D^{2/3}. \quad (\text{B.3})$$

The volumetric median drop sizes tabulated in Table B.2 are plotted in Figure B-2. The median drop sizes are correlated with sprinkler orifice diameter and water pressure as indicated in Eq. (B.3). Figure B-2 suggests that a linear relationship between  $d_m$  and  $\Delta P^{-1/3} D^{2/3}$  does exist for the presently tested geometrically similar sprinklers and conditions. The correlation equation is

$$d_m \text{ (mm)} = 1.076 \Delta P^{-1/3} D^{2/3} \text{ (kPa}^{-1/3} \text{ mm}^{2/3}\text{)}. \quad (\text{B.4})$$

OJON9.RA

TABLE B.2  
VOLUMETRIC MEDIAN DROP SIZES AND WATER DISCHARGE RATES OF SPRAYS

Spray	D(mm)	$\Delta P$ (kPa)	Water Discharge		$d_m$ (mm)
			Actual Water Discharge Rates (liters/min)	Rates Calculated by Eq. B.2 (liters/min)	
1	6.94	278	45.4	51.1	0.64
2	6.94	593	68.1	65.3	0.50
3	8.36	152	45.4	46.3	0.75
4	8.36	288	68.1	74.1	0.66
5	11.10	75	45.4	46.5	1.24
6	11.10	133	68.1	66.6	1.05
7	11.10	233	98.4	78.6	0.86

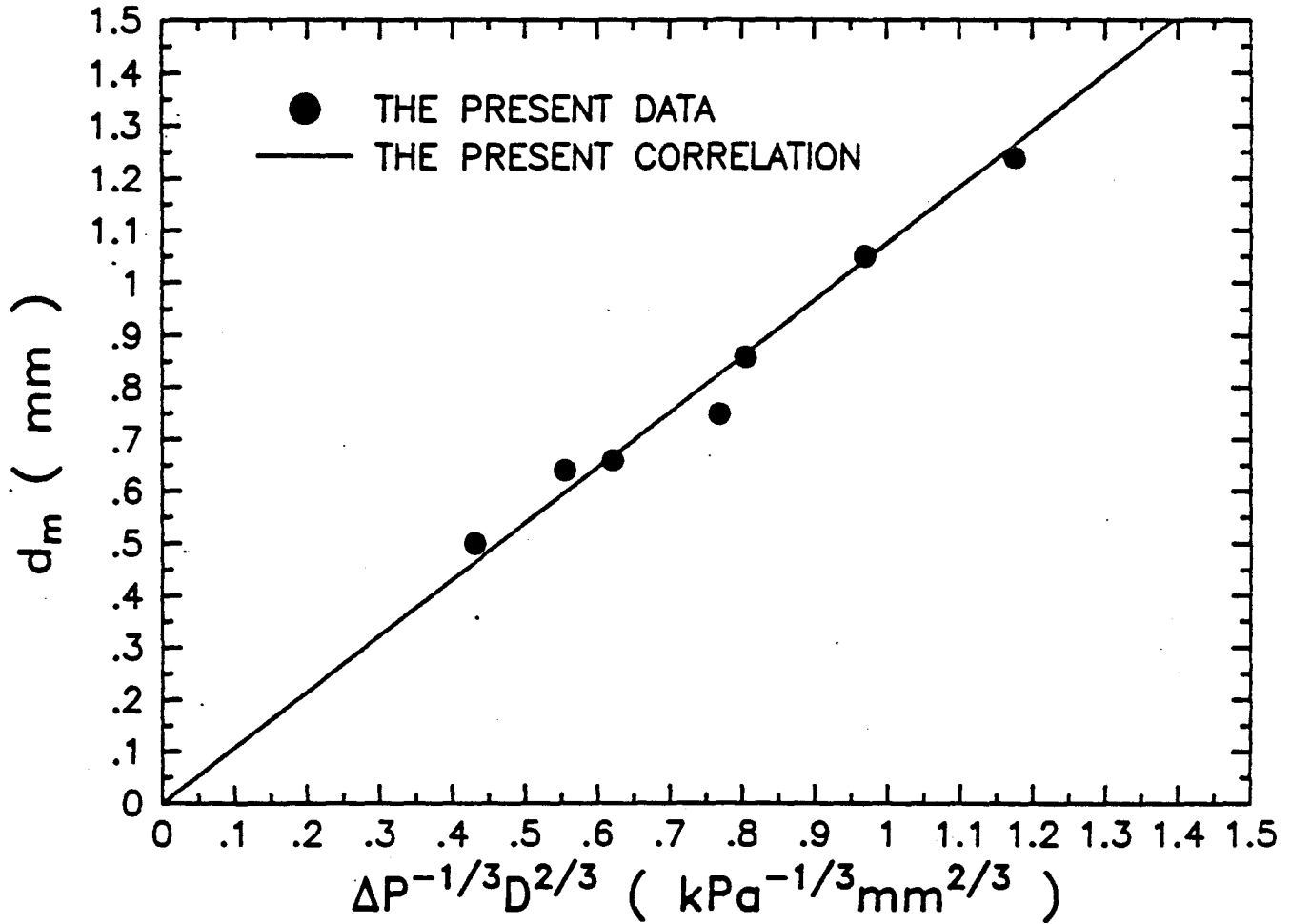


Figure B-2 Correlation of Median Drop Size with Water Pressure and Sprinkler Nozzle Diameter

U.S. DEPT. OF COMM. <b>BIBLIOGRAPHIC DATA SHEET</b> (See instructions)	1. PUBLICATION OR REPORT NO. NBS/GCR-86/515	2. Performing Organ. Report No.	3. Publication Date July 1986
4. TITLE AND SUBTITLE Spray Cooling in Room Fires			
5. AUTHOR(S) Hong-Zeng You, Hsiang-Cheng Kung, Zhanxian Han			
6. PERFORMING ORGANIZATION (If joint or other than NBS, see instructions) Factory Mutual Research 1151 Boston-Providence Turnpike Norwood, MA 02062		7. Contract/Grant No. NB83NADA4054	8. Type of Report & Period Covered Technical Report
9. SPONSORING ORGANIZATION NAME AND COMPLETE ADDRESS (Street, City, State, ZIP) National Bureau of Standards Department of Commerce Gaithersburg, MD 20899			
10. SUPPLEMENTARY NOTES  <input type="checkbox"/> Document describes a computer program; SF-185, FIPS Software Summary, is attached.			
11. ABSTRACT (A 200-word or less factual summary of most significant information. If document includes a significant bibliography or literature survey, mention it here) A series of 25 fire tests was conducted to investigate cooling in room fires by sprinkler spray. The tests were conducted in a 3.66 m x 7.32 m x 2.44 m high test room, which had a 1.22 m x 2.44 m high opening centered in one of the 3.66 m walls. The fire source was a spray fire with constant heptane flow rate, located opposite the room opening. In each test only one sprinkler was installed at the ceiling. Three geometrically similar sprinklers with nozzle diameters of 11.1 mm, 8.36 mm, and 6.94 mm were tested. Convective heat loss rate through the room opening was measured with a large fire products collector. The total heat release rate of the fire was derived from the fire products collector measurements using a carbon balance method. Heat loss rate to the ceiling and walls was measured, as well as radiative loss through the opening. Empirical correlations for the heat absorption rate of the spray and the convective heat loss rate through the room opening were established in terms of 1) total heat release rate of the fire; 2) heat loss rate to the ceiling, walls, and floor, and radiative heat loss rate through the room opening; 3) room opening area and height; 4) sprinkler discharge rate; 5) water pressure; and 6) sprinkler orifice diameter. These correlations accounted for the effects of room geometry and opening size. Experimental results obtained for a different room geometry also followed these correlations.			
12. KEY WORDS (Six to twelve entries; alphabetical order; capitalize only proper names; and separate key words by semicolons) ceilings; compartment fires; room fires; sprinklers; water sprays			
13. AVAILABILITY <input checked="" type="checkbox"/> Unlimited <input type="checkbox"/> For Official Distribution. Do Not Release to NTIS <input type="checkbox"/> Order From Superintendent of Documents, U.S. Government Printing Office, Washington, D.C. 20402. <input checked="" type="checkbox"/> Order From National Technical Information Service (NTIS), Springfield, VA. 22161		14. NO. OF PRINTED PAGES 45	15. Price \$9.95